IEEE Access
The journal for rapid open access publishing

Received September 3, 2015, accepted September 16, 2015, date of publication September 29, 2015, date of current version October 19, 2015.

Digital Object Identifier 10.1109/ACCESS.2015.2480749

Flexible Configured OFDM for 5G Air Interface

HAO LIN, (Member, IEEE)
Department of Advanced Wireless Evolution, Orange Labs, Rennes 35512, France (hao.lin@orange.com)

Part of this work was supported by the European Union within the framework of the Horizon 2020 Project FANTASTIC-5G under Grant ICT-671660.

ABSTRACT A flexible orthogonal frequency division multiplex (OFDM)-based modulation scheme is proposed under the name of Flexible Configured OFDM (FC-OFDM). It enables a flexible subband configuration and targets a multi-service scenario, which is envisioned for future 5G networks. The proposed FC-OFDM scheme provides a good compromise between the filter bank multi-carrier with offset quadrature amplitude modulation and the classical cyclic prefix-based OFDM system. The detailed system structure is illustrated in this paper, together with efficiency evaluations.

INDEX TERMS 5G, FBMC, flexibility, multicarrier modulation, multi-service, OFDM, OQAM, waveform.

I. INTRODUCTION

In cellular communication systems, the most advanced technology, i.e. LTE/LTE-A, adopts the CP-OFDM as its physical layer modulation scheme, which has proven to be very efficient for the Mobile BroadBand (MBB) service. However, moving towards future radio systems beyond 2020, it is time to ask whether the traditional fashion can effectively meet particular demands for future 5G networks. In fact, one particularity of 5G is the multi-service environment. This means that, besides the traditional MBB service, 5G cellular systems expect to offer other emerging services such as Machine Type Communications (MTC) and Vehicular to anything (V2X). Although the CP-OFDM is already well optimized for the MBB, its application in other service scenarios is still questionable and far from optimum. This is one of the reasons that several EU funded research projects have been launched to investigate alternative schemes. Among others, a leading project tackling this topic is the PHYDYAS project [1], in which the Filter Bank Multi-Carrier (FBMC) scheme, as an alternative solution to the CP-OFDM, has been extensively studied. Moreover, the advantages as well as the drawbacks are reported. To address the drawbacks, part of the solutions have also been provided [1]. After PHYDYAS, the flagship European project towards 5G, METIS, has also looked deeply at the FBMC within the context of 5G [2], where the FBMC has been seriously investigated in MTC and V2X scenarios due to its ability of supporting high mobility and relaxing synchronization constraint. According to the project conclusions [3], the FBMC is indeed advantageous and suitable for the machine type applications. However, it is also indicated that the FBMC is not fully compatible with the OFDM-based solutions, e.g. Multiple Input Multiple Output (MIMO) and pilot design, so that the LTE pilots and MIMO design cannot be straightforwardly reused in the FBMC-based systems. At this stage, one may see it as a showstopper for the FBMC scheme, since the best effort MBB, which seeks for more throughput with advanced MIMO solutions [3]–[6], will continue playing a major role in future 5G systems. Therefore, it is naturally preferred that any potential 5G waveform candidate shall prove that, besides its advantages, its usage will not create severe negative impact on the MBB service. But unfortunately, the FBMC has not yet reached this consensus.

Motivated by the above facts, we started to look for some compromised solutions. We think that in a multi-service environment it is hard to find a one-fits-all scheme; moreover, an ideal modulation scheme should be flexibly adaptable when the requested service changes. Bearing this in mind, we investigated the FC-OFDM solution because it can enable a subband-based flexible configuration, i.e. service-dedicated configuration adaptation, providing a configurable signal character. Therefore, it can well compromise the advantages and the drawbacks of both the FBMC and the CP-OFDM. For this flexibility reason, we think that it could be a good candidate for the 5G physical layer modulation scheme. This paper is organized as follows. In Sec. II, we briefly go through a high level comparison of CP-OFDM vs. FBMC, highlighting the advantages and drawbacks (or potential rooms for improvement). In Sec. III, we elaborate on the FC-OFDM scheme, including its inspiration from the so-called shaped OFDM and the transceiver design. Then, the simulation results are given in Sec. IV for further illustrating the efficiency of the proposal. In Sec. V, we provide some discussions and remarks on some issues.

Finally, some conclusions are drawn at the end. Note that the scope of this paper is limited to the downlink transmission only.

II. CP-OFDM VS. FBMC

A high level description and comparison between the CP-OFDM and FBMC is given in this section to highlight the pros and cons w.r.t. envisioned 5G services.

A. CP-OFDM

The CP-OFDM was adopted in LTE/LTE-A systems as the downlink physical layer modulation scheme and its baseband signal expression is given by

$$s_{\text{CP-OFDM}}[k] = \frac{1}{\sqrt{M}} \sum_{m=0}^{M-1} c_m e^{j\frac{2\pi m(k-L_{\text{CP}})}{M}}, \tag{1}$$

with $k \in [0, M + L_{\text{CP}} - 1]$, where c_m stands for the complex-valued QAM data symbols to be transmitted; M is the total number of subcarriers (i.e. FFT size); and L_{CP} stands for the CP duration in samples. In fact, the CP-OFDM was selected as a modern communication technology due to several advantages. To name some, it can be implemented with low complexity. The computational complexity only comes from the Inverse Fast Fourier Transform (IFFT/FFT); moreover, an appended CP effectively mimics a circular convolution between channel impulse response and the OFDM symbols, which makes the receiver processing rather simple, i.e. individual subcarrier can be processed independently due to the subcarrier orthogonality. Thus, the CP-OFDM system can not only provide good resource allocation efficiency, but also is it considered a MIMO-friendly system, which is a key enabler for 5G best effort MBB service [4]–[6]. However, the CP-OFDM is perfect only if the transmission condition is perfect, e.g. perfect synchronization and pedestrian speed; otherwise, severe performance degradation will be introduced. This is because CP-OFDM does not have localized signal spectrum confinement, which is further due to two facts: 1) the spectral leakage due to the waveform discontinuity [7], which happens at the edges of each CP-OFDM symbol; 2) the IFFT window indeed leads to a sinc-pulse character in the frequency domain with a very slow sidelobe attenuation, e.g. the second lobe attenuation is -13 dB. Therefore, a direct consequence to this is that the system needs a large guard band to control the interference level from the outer band. Moreover, in case that perfect synchronization is not retained or in high mobility circumstance, the inter-carrier interference (ICI) will appear, severely influencing the transmission quality. Such ICI will be contributed by a large amount of the modulated subcarriers due to the frequency domain sinc-pulse feature. To sum up, for the CP-OFDM scheme, the low transceiver complexity and MIMO-friendly are the main advantages. While the frequency domain sinc-pulse feature, which results in a slow sidelobe decay, is the potential improvement to be addressed.

B. FBMC

The FBMC, as an alternative scheme to the CP-OFDM, has been extensively studied [8]–[10], and the baseband modulated signal can be written as [8]

$$s_{\text{FBMC}}[k] = \sum_{m=0}^{M-1} \sum_{n\in\mathcal{Z}} a_{m,n} g[k-nN] e^{j\frac{2\pi}{M}m\left(k-\frac{D}{2}\right)} e^{j\phi_{m,n}}, \tag{2}$$

where g is the prototype filter; $D = L_g - 1$ and L_g is the length of the prototype filter g, which is normally real-valued and symmetrical; $N = M/2$ is the discrete-time offset; $\phi_{m,n}$ is an additional phase term and can be expressed as $\frac{\pi}{2}(n+m)$. The transmitted symbols $a_{m,n}$ are real-valued, which are obtained from the complex-valued QAM data symbols, taking the real and imaginary parts of these complex-valued symbols.

The key innovation of FBMC is that it relaxes the complex orthogonality to the real field in order to obtain more degrees of freedom to employ a filter being well localized in the frequency domain. Due to the real field orthogonality, real-valued symbols are to be modulated, i.e. separately transmitting the real and imaginary parts of the complex-valued QAM symbols with an offset of $T/2$, a.k.a. OQAM signaling, where T stands for the OFDM symbol duration. With the OQAM signaling, it can keep the same spectral efficiency as that of the OFDM [9]. However, also due to the OQAM signaling, the FBMC symbols are overlapped in the time domain, causing the so-called intrinsic interference, which is the essential source for its weak compatibility with LTE-based solutions; for instance as the pilot design for channel estimation [11], [12] and MIMO design [13], [14]. Thus, for the best effort MBB service of future 5G systems, if the CP-OFDM is replaced with the FBMC, many LTE-based technical components that have been developed for the traditional MBB service, e.g. the pilots and MIMO in particular, need to be redesigned, accordingly. But nevertheless, in other emerging applications, such as MMC and V2X, the good spectrum confinement feature of FBMC can bring potential gains [3]. Therefore, the good frequency isolation is an important advantage of the FBMC scheme; while the drawback is the weak compatibility with the LTE-based solution, which therefore makes it less suitable for the MBB service.

III. FLEXIBLE CONFIGURED OFDM

Based on the above analysis, we have learnt that in a multi-service context it is hard to find a one-fits-all solution. Thus, it would be good to seek for a waveform scheme that can be flexible enough to adapt the signal character to different circumstances. Bearing this in mind, we introduce a new modulation scheme, named FC-OFDM, which can configure the filter coefficients as well as the signaling mode for the multi-service adaptation. To illustrate the FC-OFDM proposal, we start with a brief introduction of the shaped OFDM concept using subcarrier filtering, followed by its extension to the FC-OFDM proposal.

IEEE Access — The journal for rapid open access publishing

A. SHAPING OFDM SYMBOL BY SUBCARRIER FILTERING

The method of shaping an OFDM symbol to an arbitrary form is based on the theory of fast convolution. It is stated that a convolution operation in the time domain corresponds to a multiplication in its frequency domain counterpart, i.e.,

$$x * y = \mathrm{IFT}(X \cdot Y), \tag{3}$$

where x and y stand for the time domain signals; while X, Y are its frequency domain counterparts and $\mathrm{IFT}(\cdot)$ stands for the inverse Fourier Transform for an infinite support. Applying this to the IFFT based system, e.g. OFDM, assuming that X is a set of the frequency domain data symbols to be mapped to the subcarriers and H is the frequency domain filter, it may yield a similar relation, i.e. if we operate a filtering between X and H (a.k.a. subcarrier filtering) before mapping to the IFFT, then we can have the following equality

$$\mathrm{IFFT}(X * H) = x \cdot h, \tag{4}$$

as long as the filtering has a circular convolution property,[1] which is equivalent to shape the conventional OFDM symbol with the form of y. This concept is not novel and was also known as the Partial Response Signaling (PRS-OFDM) [15].

Naturally, any introduced subcarrier filtering on top of the OFDM, except for the filter with unit coefficient, will cause non-orthogonality. To solve this problem, the sequence based non-linear detector, e.g. MLSE or MMSE-FDE [16], is usually used. However, as it greatly increases the receiver complexity, we prefer to look for less complex alternatives. In fact, two alternative solutions are under our investigations. 1) using OQAM signaling to relax the orthogonality to real-field; 2) utilizing a precoder before the subcarrier filtering. The first solution is indeed partially analog with the FBMC scheme. The side-effect is that, due to the OQAM signaling, the modulated multicarrier symbols in time domain are overlapped. The second solution employs a precoder before the subcarrier filtering operation, provided that the filter coefficients are known a priori. Thus normal QAM signaling can be maintained; for instance the Zero-Tail-Spread-OFDM [17], in which a Discrete Fourier Transform (DFT) precoder is employed, together with the nulled subcarriers at the edges of the precoder, can shape the OFDM symbol with a raised cosine like form. This indeed can be seen as an example of the second solution family. The advantage of this solution is that it does not introduce symbol overlapping in time domain, i.e. a block processing. While the drawback is that the usage of precoder will prevent the receiver from benefiting the channel frequency diversity, resulting in performance degradation. Moreover the scattered pilots cannot be easily inserted. In this paper, we will focus only on the first solution and leave the investigation related to the second solution in our future work.

[1] In practice, due to the insertion of guard band, the subcarriers on the two edges of IFFT are usually unmodulated, which indeed grantees a circular convolution like operation, even though a linear convolution is operated between the useful data and filter.

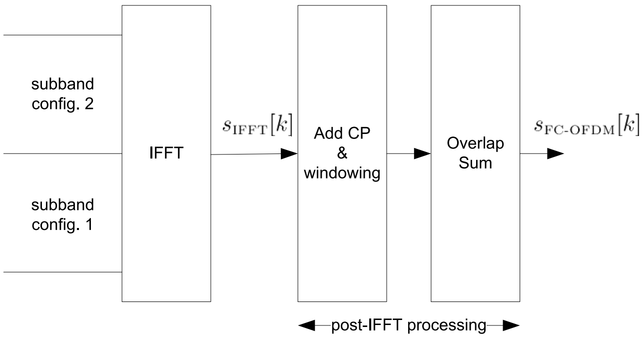

FIGURE 1. The transmitter structure of the FC-OFDM system delivering 2 services.

B. SUBBAND-WISE FLEXIBLE CONFIGURATION

In a multi-service environment, we assume that a 5G band is split into subbands over which multiple services will be delivered. The subbands may not be uniformly allocated and can, furthermore, be dynamically re-distributed over time. The idea of the FC-OFDM is to allow the base-station independently configuring the signal character within each subband according to the service needs. In Fig. 1, the FC-OFDM transmitter structure is depicted, where two subbands are assumed, and the subband-wise configuration is individually operated for each subband before the common IFFT process. Then, a post-IFFT processing is operated, including the CP appending; windowing; and overlap-sum operation. The modulated signal after the IFFT process, denoted by s_{IFFT}, is indeed aggregating two signals with different characters, i.e.,

$$s_{\mathrm{IFFT}}[k] = \sum_{n=1}^{N} s_{\mathrm{config.\,n}}[k], \tag{5}$$

with $k \in [0, M-1]$ and in the example of Fig. 1, we have $N = 2$.

With respect to the subband configurations, three possible settings are proposed in Tab. 1. In this section, we will first elaborate on the configuration set 1 and 2. While the set 3 is a particular mode and will be further discussed in Sec. IV-B.

TABLE 1. Proposed FC-OFDM configuration settings.

	filter	signaling mode	symbol duration
Set 1	$[1]$	QAM	T
Set 2	$[1, -1]$	OQAM	$T/2$
Set 3	$[1, -1]$	OQAM	T

The configuration set 1 selects an unit filter coefficient and QAM signaling with symbol duration T, which is equivalent to the OFDM symbol duration,[2] i.e. $T = MT_s$ with T_s being the sample duration. This set will produce a pure OFDM-like signal character. It implies that the QAM data symbols are directly mapped to the IFFT subcarriers allocated

[2] Note that the symbol duration T also indicates the FFT processing rate, i.e. FFT performs every T duration.

for this subband; thus the time domain modulated symbol $s_{\text{config. set 1}}[k]$ is given by

$$s_{\text{config. set 1}}[k] = \frac{1}{\sqrt{M}} \sum_{m \in (\text{subband 1})} c_m p_1[k] e^{j\frac{2\pi mk}{M}}, \tag{6}$$

with $p_1[k] = 1$, for $k \in [0, M-1]$, being the rectangular pulse shape. Therefore, the signal generated from the subband with configuration set 1 is completely compatible with the LTE-based solution, such as Cell-specific Reference Signal (CRS) design and MIMO techniques [18].

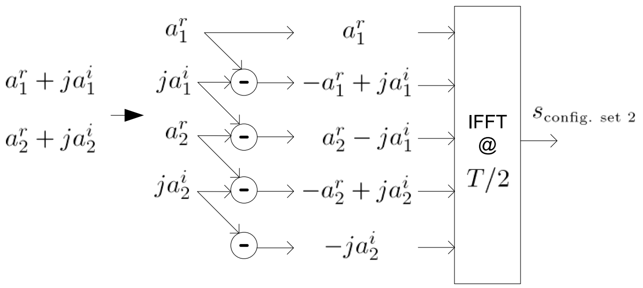

FIGURE 2. Example of configuration set 2: OQAM signaling and subcarrier filtering.

The configuration set 2, on the other hand, selects a filter with coefficients $[1, -1]$, which has a half-sine shape in the time domain. Moreover the OQAM signaling is activated. As depicted in Fig. 2, where five subcarriers are used to represent a subband, the complex-valued QAM data symbols, e.g., $c_m = a_m^r + ja_m^i$, are first separated by the real and pure imaginary parts, followed by a linear filtering between the data sequence and the filter. Thus, in the time domain after the IFFT process, the modulated symbol can be expressed as

$$s_{\text{config. set 2}}[k] = \frac{1}{\sqrt{M}} \sum_{m \in (\text{subband 2})} a_m^x p_2[k] e^{j\frac{2\pi mk}{M}}, \tag{7}$$

where a_m^x stands for the data symbols after the real-imaginary separation. For example in Fig. 2, we have $a_m^x = [a_1^r, ja_1^i, a_2^r, ja_2^i]$. Moreover, the time domain pulse shape for the configuration set 2 becomes

$$p_2[k] = \sum_{m=0}^{M-1} h_m e^{j\frac{2\pi mk}{M}}, \tag{8}$$

with

$$h_m = \begin{cases} 1 & m = 0 \\ -1 & m = 1 \\ 0 & \text{otherwise} \end{cases} \tag{9}$$

Furthermore, it is observed that the filtered symbols, except for the first and the last symbols, are still complex-valued QAM symbols, which are just a recombination of the original QAM data symbols. This indeed implies that the practical implementation does not consume any computational complexity. However, it is also noticed that, as the filter has two coefficients, the filtered symbol sequence has one additional element compared with the length of the original symbol sequence, as shown in Fig. 2. This means that an additional subcarrier will be costed to totally isolate two adjacent subbands. On the other hand, with the OQAM signaling, a doubled symbol rate, i.e. $2/T$, is needed to keep a similar spectral efficiency to that of the configuration set 1. This refers in Fig. 2 to that the IFFT needs to process at every $T/2$ time instant.

When we consider a more practical scenario, assuming that the MBB and V2X services are to be delivered in future 5G network, the base-station may select to implement the configuration set 1 in the MBB-dedicated subband for its good compatibility with LTE solutions. While the configuration set 2 could be implemented in the V2X-dedicated subband. Therefore, the first block of Fig. 1, referring to the system subband-wise configuration, can be elaborated as such shown in Fig. 3, where the IFFT runs at the smallest granularity, i.e. at $T/2$ time instant, to support the configuration set 2. In the meantime, since the symbol duration of the configuration set 1 is T, to accommodate with the configuration set 2, only the null symbols will be mapped to the IFFT inputs at every $(2n+1)T/2$ time instant with n being an integer.

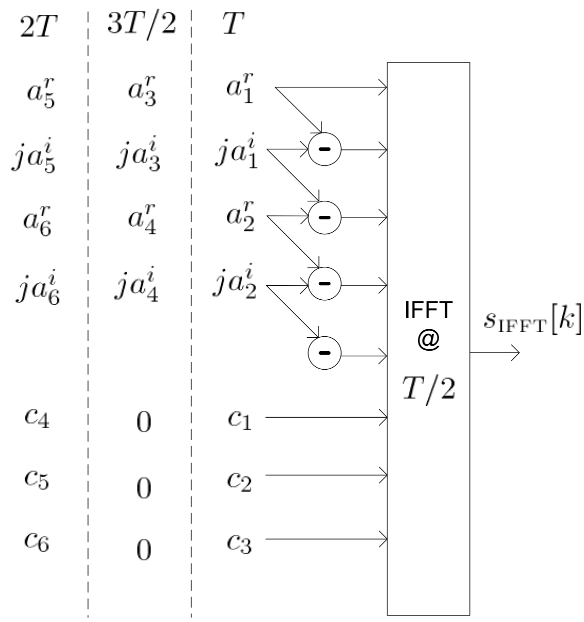

FIGURE 3. FC-OFDM subband-wise configuration: 2 subbands with configuration set 1 and 2, respectively.

The post-IFFT processing in Fig. 1 contains three steps. In the first step, a prefix and a postfix are appended to the time domain modulated symbol, i.e., $s_{\text{IFFT}}[k]$. As shown in Fig. 4, the prefix not only includes a CP but also an interval devoted to windowing called Roll-off Interval (RI); while the postfix only includes RI. Moreover, with different selected configuration settings, e.g. set 1 and 2, the post-IFFT processing for handling the prefix and postfix at $(2n)T/2$ is different from that at $(2n+1)T/2$. As can be seen from Fig. 4,

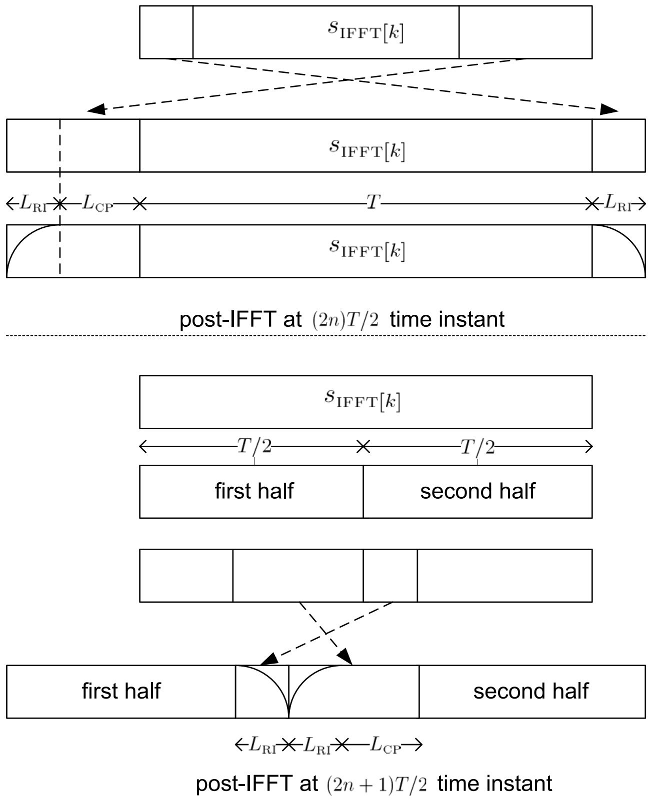

FIGURE 4. Different post-IFFT processing at time instants $(2n)T/2$ and $(2n+1)T/2$, respectively: adding prefix and postfix, followed by a windowing.

at $(2n)T/2$ time instant, the prefix, added to the head of the modulated symbol, is a duplicate of the last $L_{CP}+L_{RI}$ samples of the modulated symbol. Here L_{CP} and L_{RI} are the intervals of the CP and RI in samples, respectively. Then the postfix, copied from the first L_{RI} samples of the modulated symbol, is appended at the end. On the contrary, for the modulated symbol at $(2n+1)T/2$ time instant, the modulated symbol is first evenly cut into two portions. Then, the prefix, a duplicate of the last $L_{CP}+L_{RI}$ samples of the first half portion, is added to the beginning of the second half portion; while the postfix, a copy of the first L_{RI} samples of the second half portion, is then added to the end of the first half portion. In the second step, a windowing operation is applied on the RI samples. Here we use a raised cosine window as the window function. The final step is to implement an overlap-sum operation, following the process illustrated in Fig. 5, between the modulated symbols processed at $(2n)T/2$ and $(2n+1)T/2$ time instants. Note that the consecutive modulated symbols generated from the same time instant, e.g., either $(2n)T/2$ or $(2n+1)T/2$, do not overlap in the time domain.

C. RECEIVER DESIGN

In a downlink transmission, the receiver structure is related to the subband configuration mode. For the configuration set 1, the receiver structure is partially depicted in Fig. 6. A parallel-to-serial operation is applied to the received signal. Then two options can be envisioned: either directly take the samples corresponding to the FFT detection window, or an additional receiver windowing process is used for further reducing the inter-service interference. After that an FFT transform, which runs at every T time instant,[3] is operated. After FFT, the following processing, e.g. channel estimation, equalization, etc., is identical to the classical OFDM-based system.

With respect to the configuration set 2, a similar receiver structure is used; while the symbol duration is reduced to $T/2$. This means that the serial-to-parallel (S/P) operation needs to extract out $M+L_{CP}+2L_{RI}$ samples at every $T/2$, i.e. a reversed operation to Fig. 5. Then similar two options can be selected, i.e. directly take out the samples for FFT transform, or receiver windowing is activated. The FFT transform runs at every $T/2$ time instant. After the FFT, as shown in Fig. 7, a receiver filter, which is matched to the transmitter filter, is employed, followed by an operation that takes either the real or the imaginary part of the filter output.

IV. SIMULATION RESULTS

In this section, we evaluate the efficiency of the FC-OFDM system from different aspects, i.e. spectrum confinement, inter-service interference and robustness to mobility and Carrier Frequency Offset (CFO). In our simulations, we used LTE-like parameters: 20 MHz bandwidth, 2048 FFT size, 2 GHz carrier frequency. The CP and RI intervals are 72 and 36 samples, respectively. Moreover, we assume a multi-service scenario, where 2 services, i.e. MBB and V2X/MTC, are to be delivered from the base-station and evenly share the overall bandwidth, i.e. 50 resource blocks for each service. For the FC-OFDM configurations, we use the set 1 for the MBB subband and the set 2 for the other subband.

A. SPECTRUM CONFINEMENT

Regarding the Power Spectral Density (PSD), it is known that the classical OFDM system has a sinc-pulse shape in the frequency domain which can be expressed as $\sin(\pi v)/(\pi v)$, where v stands for the normalized frequency with the unit of subcarrier spacing $1/T$. In fact, the bad frequency localization is mainly due to that the side lobes attenuation is proportional only to $1/|v|$. However, for the FC-OFDM system with the configuration set 2, whose filter coefficients are $[1, -1]$, the subcarrier pulse-shape is transformed, after the filtering, to

$$\frac{\sin(\pi v)}{\pi v} + \frac{\sin(\pi(v+1))}{\pi(v+1)} = \frac{\sin(\pi v)}{\pi v(v+1)}. \tag{10}$$

Thus, the side lobes attenuation follows $\frac{1}{|v(v+1)|}$, which decays more rapidly than the sinc-pulse, as shown in Fig. 8. The minus sign of the second filter coefficient is used to cyclicly shift the time domain symbol by a half of symbol duration to

[3]Note that the receiver naturally cares only about a particular service subband. Therefore, to decode signal band with the configuration set 1, the receiver only needs to perform at every T time instant.

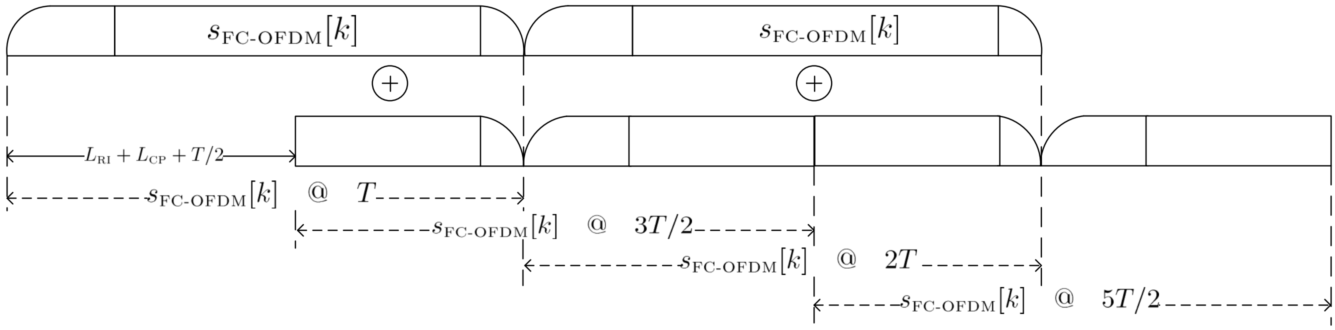

FIGURE 5. The overlap-sum operation of the FC-OFDM system: consecutive FC-OFDM symbols at time instants $(2n)T/2$ and $(2n+1)T/2$ are overlapped in time domain; while the symbols at the same rate are isolated in time domain.

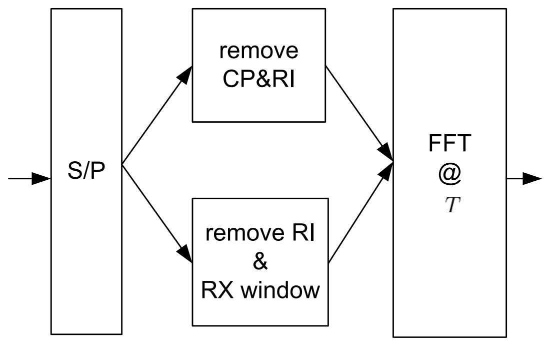

FIGURE 6. Receiver structure of FC-OFDM with the configuration set 1.

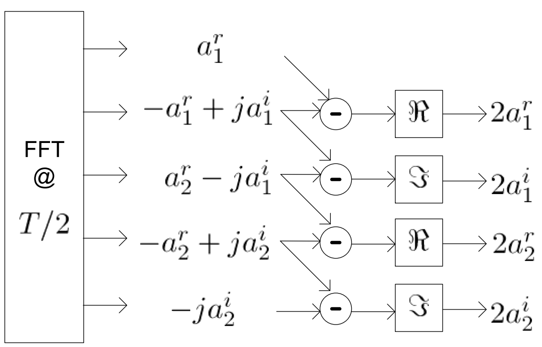

FIGURE 7. Configuration set 2: Rx filtering after FFT.

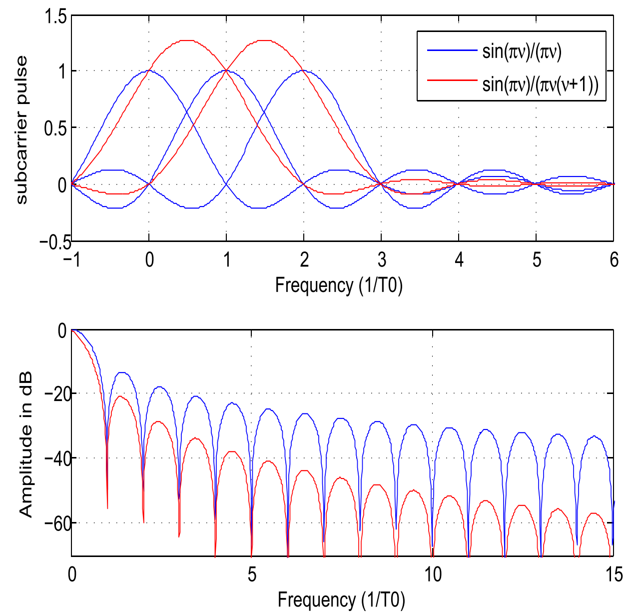

FIGURE 8. The sinc-pulse versus improved subcarrier pulse-shape.

make the side edges smoothly decay to zero, at the same time, solving the discontinuity issue.

In Fig. 9, the PSD of the FC-OFDM system is compared with the classical CP-OFDM system. The upper figure shows the PSD of the FC-OFDM with the configuration set 1 only and no transmitter windowing is employed which is equivalent to the classical CP-OFDM system. The middle figure shows a multi-service and multi-configuration FC-OFDM system without transmitter window, where two service subbands are assumed and one subband is intentionally power boosted than the other subband for the illustration purpose. It can be seen that, as explained above, the configuration set 2 gives a better spectrum confinement property than the configuration set 1. However, when the transmitter windowing process is not operated, the overall system spectrum confinement is limited by the subband with the configuration set 1. Moreover, when the CP is added, the PSD of the subband with the configuration set 2 becomes worse, which is owing to the waveform discontinuity issue. Finally, in the lower figure, once the transmitter window is employed the discontinuity issue can be removed, which effectively improves the overall system spectrum confinement.

B. INTER-SERVICE INTERFERENCE

Naturally, when different configurations are implemented for different subbands, in particular for the case where QAM and OQAM signaling are simutanouusly used for different subbands, there is an interference between subbands. This is called the inter-subband interference or inter-service interference. In the following, we analyze the interference power between different service subbands. Similar to the previous section, 2 subbands (or services) share the overall band and

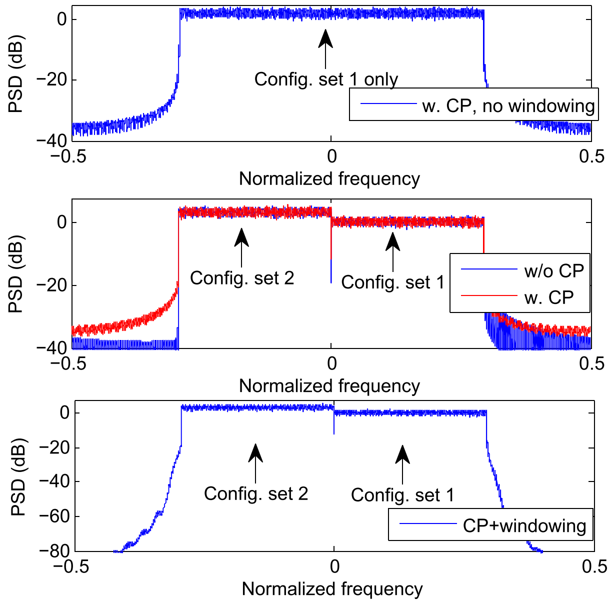

FIGURE 9. The PSD comparison: the upper figure is configured only by the set 1; the middle figure is configured by 2 sets but without Tx windowing; the lower figure is configured by 2 sets with both CP and Tx windowing.

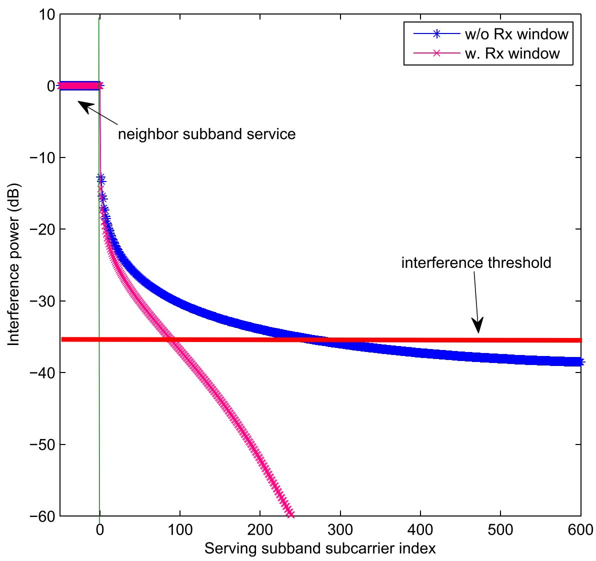

FIGURE 10. Observed interference power: serving subband has the configuration set 1 and neighbor subband has the configuration set 2.

the configuration set 1 and 2 are selected for these subbands, respectively (c.f. Fig. 3). The inter-service interference is expressed in decibels and it is caused by the neighbor service subband but observed from the serving service subband. The simulation results are depicted in Figs. 10 and 11, where we set zero power-offset between two subbands signal, i.e. equivalent transmit power over two subbands. It can be seen from Fig. 10, when the serving subband is configured with the set 1 and no receiver windowing is used, the major interference presents at the subband edge close to the neighbor subband. If we take −35 dB as the interference sensitivity threshold, then half of the bandwidth will suffer

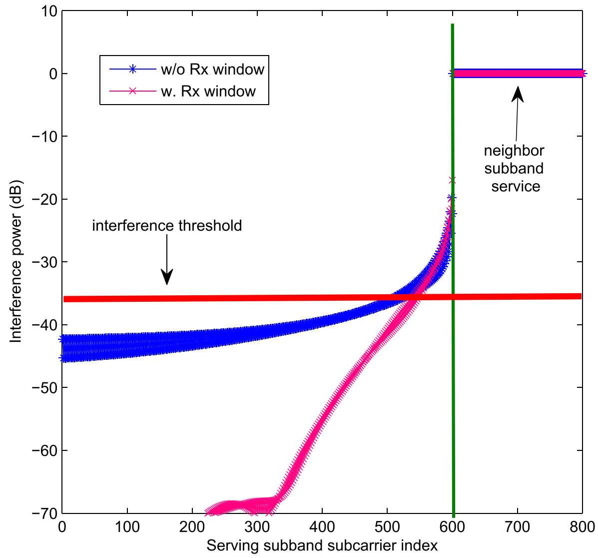

FIGURE 11. Observed interference power: serving subband has the configuration set 2 and neighbor subband has the configuration set 1.

from the performance degradation, since the interference curve intersects the threshold curve at the point of half band. Nevertheless, once the receiver windowing is employed, the interference power is remarkably reduced and only the edge subcarriers are impacted by the interference. Differently, when the serving subband is configured with the set 2, as shown in Fig. 11, most of the band will receive the interference with a level being already under the sensitivity threshold. This is because the receiver filtering, c.f. Fig. 7, can partially reduce the interference. Although the additional receiver windowing can further reduce the interference level, it cannot improve the performance of the edge subcarriers that are close to its neighbor subband. Next, we propose two solutions to solve this issue. The first solution is to leave the network to schedule the user with more robust Modulation and Coding Scheme (MCS) to this interference-limited subcarriers. The second solution is to insert a protection band between the 2 subbands. Thus, the interference at the edge subcarriers can be relieved when the 2 subbands are further apart. A common practical way of introducing a protection band is to insert some null subcarriers between the 2 subbands. However, this will reduce the spectral efficiency. Here we propose a compromised solution by inserting a protection band, within which a third configuration mode is selected and data symbols can be transmitted over these subcarriers. This configuration selects the same filter coefficient as the configuration set 2 but a half-rate OQAM signaling is used with symbol duration T, which is named thereby the configuration set 3 (c.f. Tab. 1). Thus, including the protection band configuration, the subband-wise configuration will look like Fig. 12. The advantage of using the configuration set 3 in the protection band is that the symbols transmitted in this protection band is orthogonal to the other 2 subbands. In Fig. 13, we show the interference level when the serv-

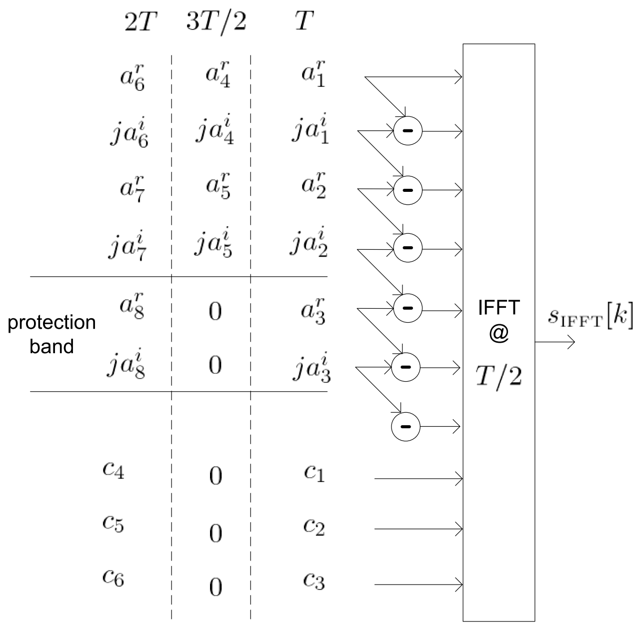

FIGURE 12. FC-OFDM subband-wise configuration: set 1, 2 and 3; The configuration set 3 is used in the protection band.

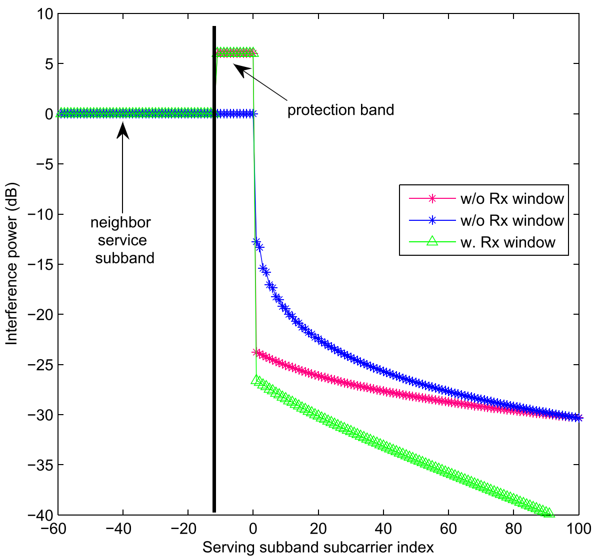

FIGURE 13. Observed interference power: serving subband has the configuration set 2 and neighbor subband has the configuration set 1 and protection band has the configuration set 3.

ing subband is configured with set 1 and 12 subcarriers (equivalent to 1 resource block) are used as the protection band. Moreover, the transmit power in the protection band is boosted for the illustration purpose. It can be seen that the interference at the edge subcarriers of the serving service subband is greatly reduced, even without the receiver windowing. For example the interference on the subcarrier placed at the most edge of the the serving subband is reduced from −12 dB to −24 dB. When the receiver windowing is employed, further interference reduction can be realized over the all subband. Regarding the spectral efficiency loss,

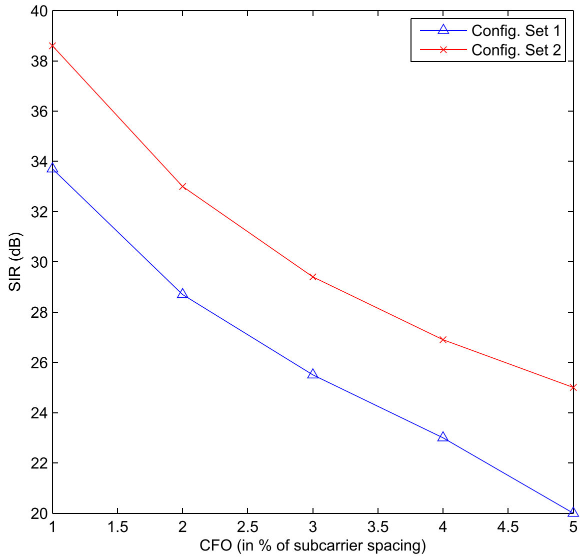

FIGURE 14. CFO immunity comparison: the configuration set 1 versus set 2.

the proposed configuration set 3 gives a good compromise between the zero guard band and the full guard band. Assuming N subcarriers are used as the protection band, the effective spectral efficiency loss is equal to that of $N/2$ null subcarriers. While, its interference isolation capacity is equivalent to that of N null subcarriers, as it is indeed the number of the inserted subcarriers for the subbands separation.

C. ROBUSTNESS TO MOBILITY AND CFO

Next we show the interest of enabling flexible configuration in the FC-OFDM system. The configuration set 1 is naturally suitable for MBB service. While for other emerging applications such as low cost MTC and high mobility V2X, the configuration set 2 can provide better performance. In this section, we evaluate the robustness of the configuration set 2 against mobility and Carrier Frequency Offset (CFO). The former reflects the potential advantage in the V2X service and the latter would be interested by the low cost MTC devices. The comparison is evaluated in terms of the Signal to Interference Ratio (SIR). For the CFO immunity comparison, the tested CFO goes up to 5% of the subcarrier spacing. It can be seen from Fig. 14 that the configuration set 2 outperforms the set 1 and the SIR gain amounts approximately to 5 dB. For the mobility robustness comparison, we use a Rayleigh fading channel with Jakes model and the carrier frequency is 2 GHz and an ideal channel estimation is assumed in our simulation. The comparison results in terms of SIR versus velocity (up to 500 Kmph) are reported in Fig. 15. It is observed that the configuration set 2 can also provide around 5 dB gain compared with the configuration set 1 in the high speed case. Therefore, it confirms the potential interest of using multi-configuration for multi-service. In future 5G networks, the MBB service will remain a major role. Thus the configuration set 1 might need to be constantly used. Nevertheless, once there is a request for emerging services, the FC-OFDM can

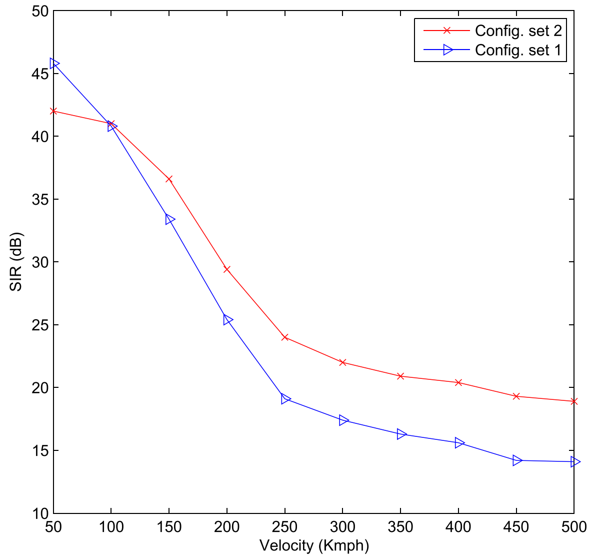

FIGURE 15. Mobility immunity comparison: the configuration set 1 versus set 2.

efficiently be adapted to address these services and, at the same time, coexist with the MBB service. This is the beauty of the proposed FC-OFDM scheme.

V. DISCUSSIONS

In this section, we discuss some questions that might interest the readers and may further motivate our future work. The selected points to be discussed include: What is the FC-OFDM complexity? Why the FC-OFDM is a compromised solution? What is the spectral efficiency of the FC-OFDM system? And are there any other configuration setting possibilities?

A. FC-OFDM COMPLEXITY

The complexity increase at the base-station side is mainly due to the doubled FFT rate. Therefore, when two services, with different configurations, are delivered in the network, the base-station complexity is increased up to a factor of 2. Nevertheless, during the time when the emerging scenarios do not present, the base-station can shift to single-configuration system, e.g. only supporting MBB service. Thus, the complexity increase at the base-station is only due to the windowing process, which is completely negligible. On the receiver side, if the receiver attempts to decode the configuration set 1 signal, the complexity increase, compared to OFDM-based receiver, is negligible; while for the configuration set 2 device, the $T/2$ processing rate will increase complexity by a factor of 2. To conclude, for the FC-OFDM system, the maximum complexity increase compared to the CP-OFDM is a factor of 2; but nevertheless, it should be noted that such complexity increase happens only when the configuration set 2 is activated to address some corner cases. Hence, it is a sporadic complexity increase.

B. COMPROMISING FBMC AND CP-OFDM

The proposed configuration set 1 and 2 for the FC-OFDM are indeed a compromised solution of the FBMC and the CP-OFDM. To be more specific, compared to the CP-OFDM, the FC-OFDM uses an additional windowing process that significantly shapes the signal spectrum confinement. Therefore, the compromise is to trade a portion of the CP for the window interval RI for improving the spectrum localization. While comparing with the FBMC, a CP is employed for the FC-OFDM system, which normally is not needed in the classical FBMC system. Therefore, we trade the spectral efficiency for enabling that signals with different characters, e.g. FBMC-like and CP-OFDM-like, can be processed at the same time and share a common IFFT. This not only keeps the modulation complexity at a low level, but also does it provide the base-station with a high degree of flexibility for subband configuration.

C. FC-OFDM SPECTRAL EFFICIENCY

Regarding the spectral efficiency, the proposed FC-OFDM system does send redundant samples in the time domain for the CP and RI. Thus, at a quick glance, it should lead to a similar spectral efficiency to that of the CP-OFDM system. But nevertheless, due to the enhanced spectrum confinement, more subcarriers can indeed be practically used for data transmission. For instance, for LTE numerology of 20 MHz bandwidth [18], due to the spectrum mask regulation, 100 resource blocks are allowed to transmit data symbols, resulting the effective bandwidth in 18 MHz. With the FC-OFDM, the effective bandwidth can therefore be increased more closely to 20 MHz, e.g. up to 19.8 MHz by modulating additional 10 resource blocks (120 subcarriers), immediately yielding a spectral efficiency gain by around 10%. Although the introduced subcarrier filtering will cost 1 subcarrier, and so as for the employment of the protection band, the FC-OFDM can still outperform the CP-OFDM in terms of the spectral efficiency.

D. OTHER FC-OFDM CONFIGURATION SETTINGS

Three configuration settings have been proposed in this paper. However, as previously stated, the configuration is not limited to these three modes. Indeed, some hints have already been provided in Sec. III-A, where the precoder solution can eventually be considered as additional configuration mode for the FC-OFDM system. We will continue looking at the joint precoder and filter design in our future work. But nevertheless, due to the signaling overhead constraint, we believe that in practice the number of the configuration settings should anyway be limited to a reasonable number, e.g. up to 4 possibilities.

VI. CONCLUSIONS

In this paper, we have illustrated the fact that in a multi-service environment with diverse requirements, it would be hard to find a uniformed solution that fits all different scenarios. Thus, we have proposed a flexible configured OFDM (FC-OFDM) scheme, which can flexibly configure different subbands characters. Therefore it could be suited for 5G multi-service environment. In addition, three configuration settings have also been presented, which indeed compromise the advantages and drawbacks of the CP-OFDM and FBMC schemes. Naturally, the flexibility of the proposed FC-OFDM concept should not be limited only by the presented configuration settings. Our future research will continue looking for potential configuration possibilities that may provide more robustness in the 5G context.

ACKNOWLEDGEMENTS

The author would like to acknowledge the contributions of their colleagues in FANTASTIC-5G.

REFERENCES

[1] *PHYDYAS Project FP7*. [Online]. Available: http://www.ict-phydyas.org/, accessed Jan. 10, 2008.
[2] *Deliverable D2.4: Proposed Solutions for New Radio Access*, document ICT-317669-METIS/D2.4, METIS, Mar. 2015.
[3] *Deliverable D6.5: Report on Simulation Results and Evaluations*, document ICT-317669-METIS/D6.5, METIS, Mar. 2015.
[4] *Further Advancements for E-UTRA Physical Layer Aspects*, document 3GPP TR 36.814, 3GPP Technical Specification Group Radio Access Network, Mar. 2010.
[5] R. Irmer *et al.*, ''Coordinated multipoint: Concepts, performance, and field trial results,'' *IEEE Commun. Mag.*, vol. 49, no. 2, pp. 102–111, Feb. 2011.
[6] F. Rusek *et al.*, ''Scaling up MIMO: Opportunities and challenges with very large arrays,'' *IEEE Signal Process. Mag.*, vol. 30, no. 1, pp. 40–60, Jan. 2013.
[7] F. J. Harris, ''On the use of windows for harmonic analysis with the discrete Fourier transform,'' *Proc. IEEE*, vol. 66, no. 1, pp. 51–83, Jan. 1978.
[8] P. Siohan, C. Siclet, and N. Lacaille, ''Analysis and design of OFDM/OQAM systems based on filterbank theory,'' *IEEE Trans. Signal Process.*, vol. 50, no. 5, pp. 1170–1183, May 2002.
[9] H. Bölcskei, ''Orthogonal frequency division multiplexing based on offset QAM,'' in *Advances in Gabor Analysis* (Applied and Numerical Harmonic Analysis). Boston, MA, USA: Birkhäuser, 2003, pp. 321–352.
[10] M. Bellanger, ''FBMC physical layer: A primer'' ICT-PHYDYAS, Tech. Rep., 2010, pp. 1–31.
[11] J.-P. Javaudin, D. Lacroix, and A. Rouxel, ''Pilot-aided channel estimation for OFDM/OQAM,'' in *Proc. 57th IEEE Semiannu. Veh. Technol. Conf. (VTC-Spring)*, Apr. 2003, pp. 1581–1585.
[12] Z. Zhao, N. Vucic, and M. Schellmann, "A simplified scattered pilot for FBMC/OQAM in highly frequency selective channels," in *Proc. 11th Int. Symp. Wireless Commun. Syst. (ISWCS)*, Aug. 2014, pp. 819–823.
[13] R. Zakaria and D. Le Ruyet, ''On interference cancellation in Alamouti coding scheme for filter bank based multicarrier systems,'' in *Proc. 10th Int. Symp. Wireless Commun. Syst. (ISWCS)*, Aug. 2013, pp. 1–5.
[14] M. Caus and A. I. Perez-Neira, ''Multi-stream transmission for highly frequency selective channels in MIMO-FBMC/OQAM systems,'' *IEEE Trans. Signal Process.*, vol. 62, no. 4, pp. 786–796, Feb. 2014.
[15] V. Vadde and S. Gray, ''Partial response signaling for enhanced spectral efficiency and RF performance in OFDM systems,'' in *Proc. Global Telecommun. Conf. (GLOBECOM)*, vol. 5. 2001, pp. 3120–3124.
[16] V. Vadde, ''Partial response signaling for equalization of OFDM systems in severe multipath channels,'' in *Proc. Conf. Rec. 35th Asilomar Conf. Signals, Syst., Comput.*, vol. 2. Nov. 2001, pp. 1601–1605.
[17] G. Berardinelli, F. M. L. Tavares, T. B. Sorensen, P. Mogensen, and K. Pajukoski, "Zero-tail DFT-spread-OFDM signals," in *Proc. IEEE Globecom Workshops (GC Wkshps)*, Dec. 2013, pp. 229–234.
[18] S. Sesia and I. Toufik, and M. Baker, *LTE—The UMTS Long Term Evolution: From Theory to Practice*. New York, NY, USA: Wiley, 2009.

HAO LIN received the Ph.D. degree in communication and electronics from the Ecole National Supérieure des Télécommunications Paris, France, in 2009. Since 2010, he has joined Orange Labs, Rennes, as a Research Engineer. His research interests include multi-carrier modulation and signal processing for communications. He serves as the Task Leader in FP7-METIS and Work-Package Leader of Fantastic-5G projects.